

Weak charge pion production puzzles

Jan T. Sobczyk

Wrocław University

Wrocław/Fermilab, August 21, 2014

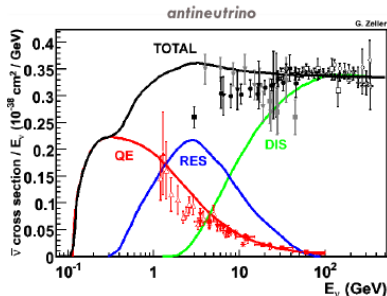
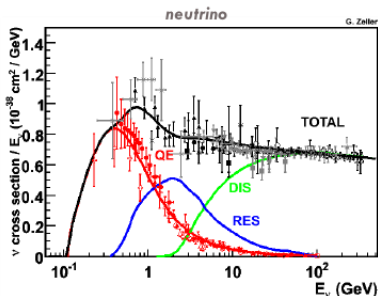


Outline:

- introduction
- puzzle 1: ANL and BNL normalization
- puzzle 2: neutron versus proton π^+ production
- puzzle 3: MiniBooNE π^+ production data
- puzzle 4: MiniBooNE versus MINERvA π^+ production data



Basic interactions modes – vocabulary



Sam Zeller; based on P. Lipari et al

CCQE is $\nu_\mu n \rightarrow \mu^- p$, or $\bar{\nu}_\mu p \rightarrow \mu^+ n$.

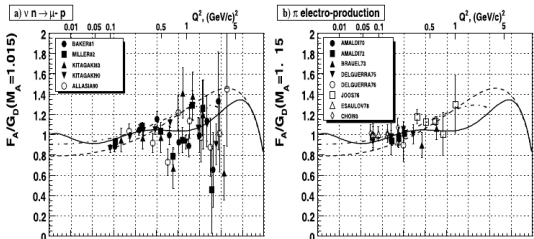
RES stands for **resonance region** e.g. $\nu_\mu p \rightarrow \mu^- \Delta^{++} \rightarrow \mu^- p \pi^+$;
one often speaks about **SPP** - single pion production

DIS stands for: more inelastic than **RES**.

In the ~ 1 GeV region **CCQE** and **RES** are most important.



CCQE and MEC under control?



- older M_A measurements indicate the value of about 1.05 GeV
- independent pion production arguments lead to the similar conclusion

The experimental data is consistent with dipole axial FF and $M_A = 1.015$ GeV.

A. Bodek, S. Avvakumov, R. Bradford, H. Budd

In the near future there should be reliable (5%?) theoretical computations of weak nuclear response (Euclidean response or sum rules) in the QE peak region for carbon, including both one body and two body current contributions.

J. Carlson, R. Schiavilla, A. Lovato et al



Why do we need to understand RES?

- often these are background events
 - if π is absorbed they mimic CCQE (used to measure ν oscillation signal)
 - NC π^0 decay into 2γ and can be confused with ν_e
- pion production channels important at LBNE energies
- theoretical interest, hadronic physics



Neutrino SPP channels

For neutrinos there are three charged current (CC) channels:

$$\nu_l p \rightarrow l^- p \pi^+,$$

$$\nu_l n \rightarrow l^- n \pi^+,$$

$$\nu_l n \rightarrow l^- p \pi^0.$$

The name RES (resonance) reflects an observation that most of the cross section comes from resonance excitation, in the ~ 1 GeV energy region mostly of Δ resonance:

$$\nu_l p \rightarrow l^- \Delta^{++} \rightarrow l^- p \pi^+,$$

$$\nu_l n \rightarrow l^- \Delta^+ \rightarrow l^- n \pi^+,$$

$$\nu_l n \rightarrow l^- \Delta^+ \rightarrow l^- p \pi^0.$$

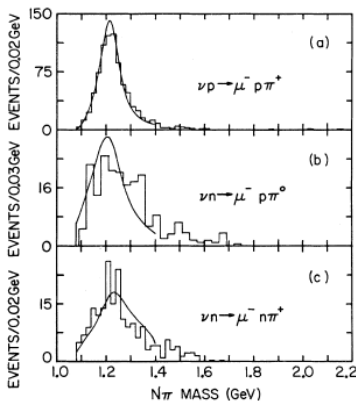
Assuming that the only mechanism is Δ excitation, isospin rules tell us that the cross sections ratio is 9:1:2.

Very little is known about weak current excitation of heavier resonances.

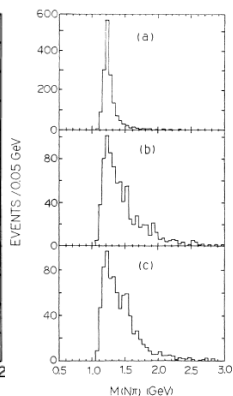


Δ resonance in the weak pion production data

Below, distributions of events in invariant hadronic mass, from old bubble chamber experiments:



ANL



BNL

The $p\pi^+$ channel is overwhelmingly dominated by the Δ excitation but in other two channels the situation is more complicated.

Theoretical models must include a non-resonant background.

An experimental status of RES – overview:

- there are ~ 30 years old deuterium (plus a small fraction of hydrogen – 105 events) bubble chamber data from Argonne (ANL) and Brookhaven (BNL) experiments
 - there is a lot of discussion if ANL and BNL data are consistent in $p\pi^+$ channel
 - problem of consistency between three SPP channels
- there are more recent measurements done on nucleus targets (mostly carbon)
 - difficult to disentangle nuclear (FSI) effects
 - there is an interesting tension between MiniBooNE and very recent MINERvA data

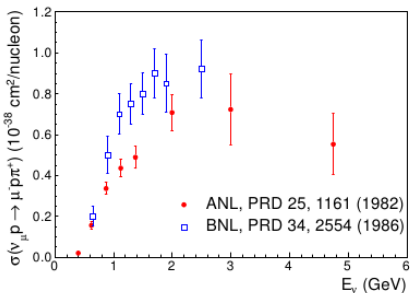
Altogether ...

- ... we can speak about **weak pion production puzzles**.



ANL and BNL data

It is often claimed there is a tension between both data sets:



In the data there is no cut on W .

An apparent discrepancy at $E_\nu \sim 1.5$ GeV.

from Phil Rodrigues

It seems however, that both experiments did not pay much attention to overall flux normalization error.



Normalization in ANL

Below, results for $\frac{d\sigma}{dQ^2}$ from ANL experiments.

Q^2	$d\sigma/dQ^2$	$\Delta\sigma/\sigma$	N (events)	$1/\sqrt{N}$
0.01-0.05	0.527 ± 0.079	15%	51.4	13.9%
0.05-0.1	0.724 ± 0.084	11.6%	94.5	10.3%
0.1-0.2	0.656 ± 0.058	8.8%	158.4	7.9%
0.2-0.3	0.546 ± 0.052	9.5%	133.3	8.7%
0.3-0.4	0.417 ± 0.045	10.8%	99.2	10%
0.4-0.5	0.307 ± 0.038	12.4%	70.6	11.9%
0.5-0.6	0.215 ± 0.032	14.9%	54.8	13.5%
0.6-0.8	0.138 ± 0.018	13.0%	66.2	12.3%
0.8-1.0	0.069 ± 0.013	18.8%	33.4	17.3%

The patterns of **reported total error** and **statistical errors** are identical, with an overall rescaling by ~ 1.08 . Translated into quadrature it gives **other error** as small as 3.9 – 7.3%.



Normalization in ANL

Total ANL cross sections have errors from 8.9% (in the bin (0.75 – 1) GeV) up. It seems they include mostly statistical errors as well.

Another minor point:

In order to investigate Δ region one can use ANL data with an appropriate cut on invariant hadronic mass $W < 1.4$ GeV. The same is impossible with the BNL data.

A realistic assumption is that the flux normalization errors in both experiments are: 20% for ANL and 10% for BNL.

Re-analysis of the ANL and BNL data with a flux renormalization error and deuteron effects was done in

Graczyk, Kiełczewska, Przewłocki, JTS, Phys. Rev D80 093001 (2009).



ANL and BNL data re-analysis

$$\chi^2 = \sum_{i=1}^n \left(\frac{\sigma_{th}^{diff}(Q_i^2) - p\sigma_{ex}^{diff}(Q_i^2)}{p\Delta\sigma_i} \right)^2 + \left(\frac{p-1}{r} \right)^2,$$

$\sigma_{tot-exp}$ and σ_{tot-th} are the experimental and theoretical flux averaged cross sections measured and calculated with the same cuts, r is a normalization error, p is an unknown flux correction normalization factor (to be found in the fit).

D'Agostini, Nucl. Instrum. Meth. A346 (1994) 306.

The fit was done to $\nu_{\mu}p \rightarrow \mu^{-}p\pi^{+}$ channel with a model that contained only Δ^{++} , and no non-resonant background. The results were surprising: **both data sets are in agreement!** Best fit values of renormalization factors were found to be: $p_{ANL} = 1.08 \pm 0.1$ and $p_{BNL} = 0.98 \pm 0.03$.



ANL (left) and BNL (right) data re-analysis

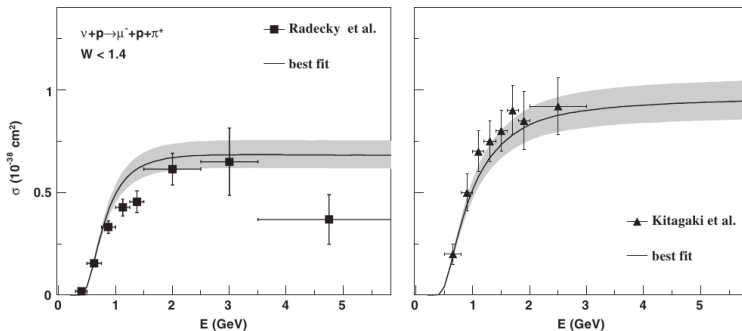
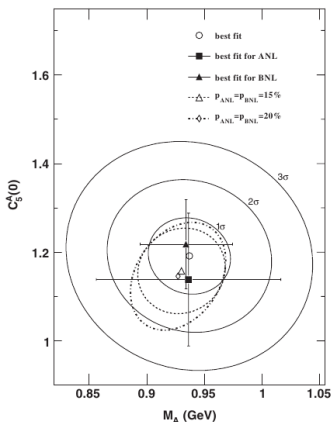


FIG. 5. Total cross section for $\nu + p \rightarrow \mu^- + p + \pi^+$. In the left panel the ANL data [5] with the cut $W = 1.4$ are shown (black squares), while the right panel presents the BNL data [42] (without cuts in W)—black triangles. The overall normalization error is not plotted. The best fit curves were obtained with a corresponding cut in W . The theoretical curves were obtained with dipole parametrization Eq. (32) with $M_A = 0.94 \text{ GeV}$ and $C_3^A(0) = 1.19$. The shaded areas denote the 1σ uncertainties of the best fit. The theoretical curves are not modified by the deuteron correction effect.



ANL and BNL data re-analysis

Parameter goodness of fit also showed a good agreement between both data sets.



The idea **parameter goodness of fit** is to compare separate ANL and BNL fits with a joint fit.

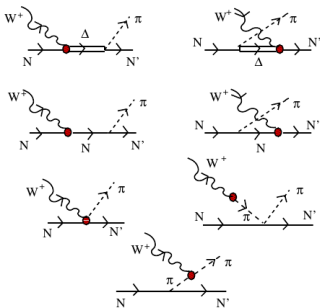
Maltoni, Schweps



Neutron SPP channels, non-resonant background

As seen before in the neutron SPP channels non- Δ contribution is very important.

A possible strategy: take a model based on Chiral Field Theory:



Hernandez, Nieves, Valverde, Phys.Rev. D76 (2007) 033005

The same set of diagrams is used in MEC computations.

Neutron SPP channels, non-resonant background

In phenomenological studies one makes a fit to $N \rightarrow \Delta$ transition matrix element form-factors:

$$\begin{aligned} \langle \Delta^{++}(p') | V_\mu | N(p) \rangle &= \sqrt{3} \bar{\Psi}_\lambda(p') \left[g_\mu^\lambda \left(\frac{C_3^V}{M} \gamma_\nu + \frac{C_4^V}{M^2} p'_\nu + \right. \right. \\ &\quad \left. \left. \frac{C_5^V}{M^2} p_\nu \right) q^\nu - q^\lambda \left(\frac{C_3^V}{M} \gamma_\mu + \frac{C_4^V}{M^2} p'_\mu + \frac{C_5^V}{M^2} p_\mu \right) \right] \gamma_5 u(p) \\ \langle \Delta^{++}(p') | A_\mu | N(p) \rangle &= \sqrt{3} \bar{\Psi}_\lambda(p') \left[g_\mu^\lambda \left(\gamma_\nu \frac{C_3^A}{M} + \frac{C_4^A}{M^2} p'_\nu \right) q^\nu - \right. \\ &\quad \left. q^\lambda \left(\frac{C_3^A}{M} \gamma_\mu + \frac{C_4^A}{M^2} p'_\mu \right) + g_\mu^\lambda C_5^A + \frac{q^\lambda q_\mu}{M^2} C_6^A \right] u(p). \end{aligned}$$

$\Psi_\mu(p')$ is Rarita-Schwinger field, and $u(p)$ is Dirac spinor.

Typically, one fits values of $C_5^A(0)$ and M_A , where $C_5^A(Q^2) = \frac{C_5^A(0)}{\left(1 + \frac{Q^2}{M_A^2}\right)^2}$,

imposing reasonable conditions on remaining ones. Vector FF are taken from electroproduction experiments.



Neutron SPP channels, non-resonant background

Such a study has been done recently using ANL data with a cut $W < 1.4$ GeV. Deuteron effects in plane wave impulse approximation (neglecting FSI) are included.

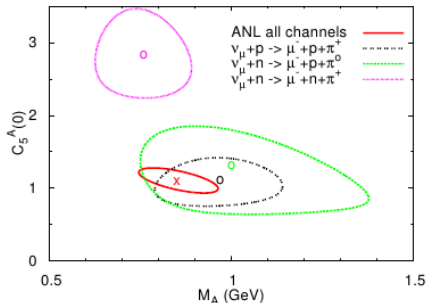


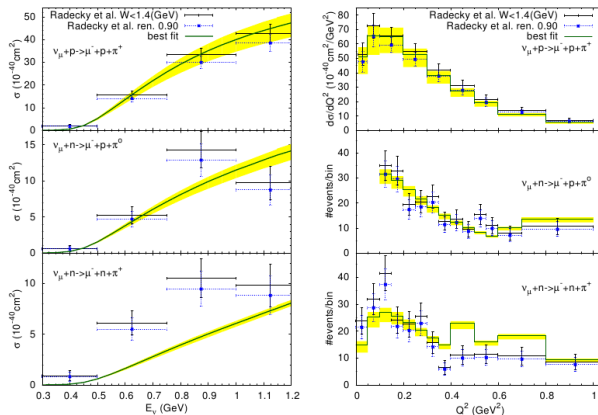
FIG. 5. (Color online) 1σ uncertainty contours for fits on deuteron target.

Graczyk, Źmuda, JTS, arXiv:1407.5445[hep-ph]

The $n\pi^+$ channel prefers much larger value of $C_5^A(0)$, and seems to be inconsistent with the other two.



Neutron SPP channels, non-resonant background

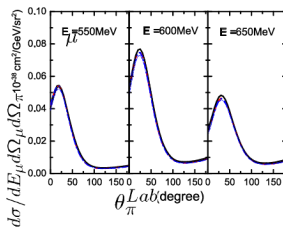
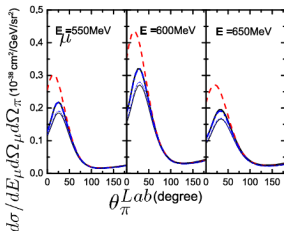
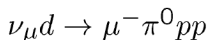
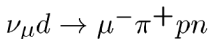


In the $n\pi^+$ channel the measured cross section is much larger than the calculated one.



Neutron SPP channels, non-resonant background

A recent study by Toru Sato shows that deuteron FSI effects are not negligible in the $p\pi^+$ and $n\pi^+$ channels in the low θ_π region.



- Impulse
- · - · Impulse + NN
- Impulse+NN+piN

$$E_\nu = 1 \text{ GeV}$$

$$\theta_\mu = 25^\circ$$

~ Delta-QF kinematics

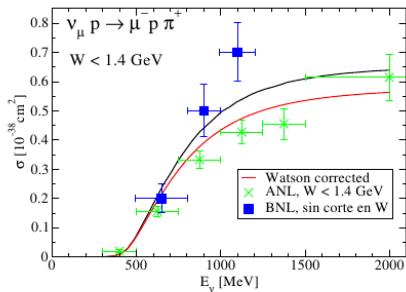
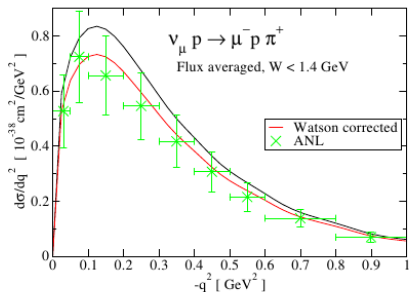
Neutron SPP channels, non-resonant background

What goes wrong may be a lack of unitarity in the model.

- unitarity and time invariance relate weak pion production matrix element phase with a pion-nucleon interaction matrix element (Watson theorem)
- study done by L. Alvarez-Ruso, E.Hernandez, J. Nieves, M. Valverde, and M.J. Vicente Vacas
- a few details in backup slides.



Watson theorem



This suggest larger $C_5^A(0)$ values are needed

E. Hernandez, CETUP*2014



Nuclear target SPP measurements

- typically, one measures cross section for 1π in the final state
- not the same as free nucleon SPP
 - pion absorption
 - pion charge exchange

Important advantage vrt old measurements:

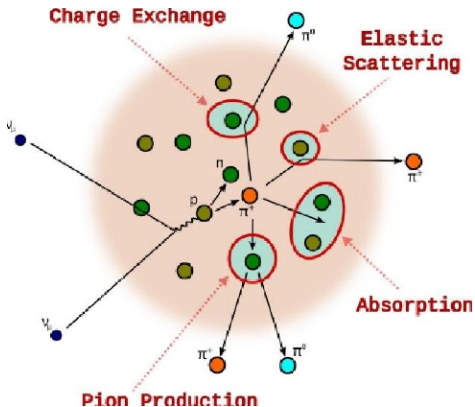
- much better statistics

Theoretical computations should include Δ in-medium self energy broadening, see backup slides.



Final state interactions:

What is observed are particles in the final state.



Pions...

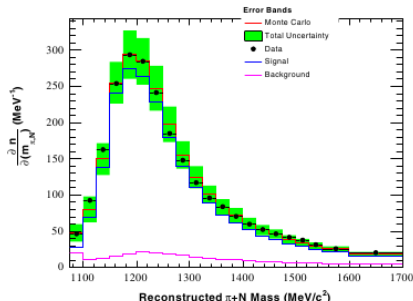
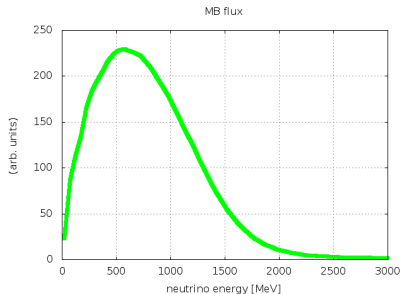
- can be absorbed
- can be scattered elastically
- (if energetically enough) can produce new pions
- can exchange electric charge with nucleons

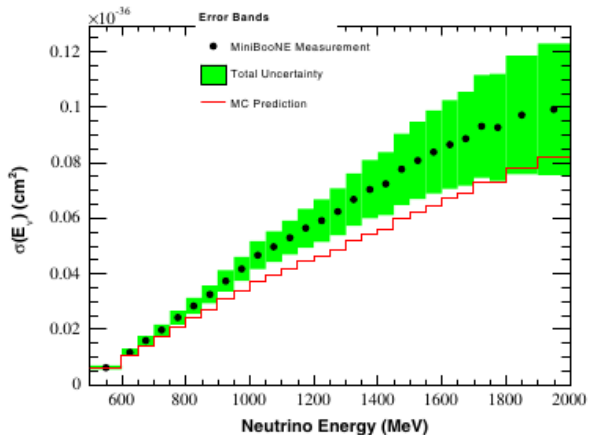
from T. Golan



MiniBooNE CC π^+ production measurement

- target is CH_2
- flux peaked at 600 MeV, without high energy tail \Rightarrow the relevant dynamics is in the Δ region
- coherent π^+ production is a part of the signal
- signal defined as $1\pi^+$ and no other pions in the final state.

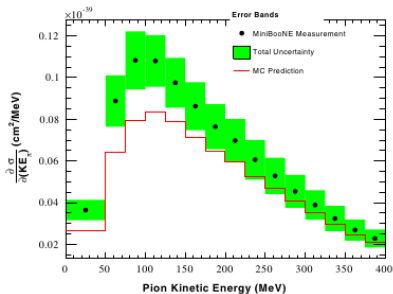


MiniBooNE CC π^+ production measurement

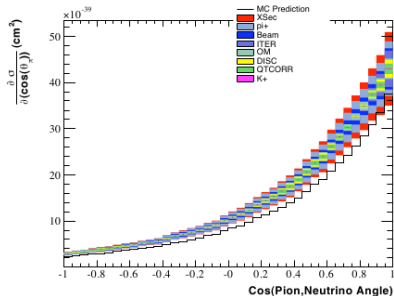
A. A. Aguilar-Arevalo et al [MiniBooNE] PRD 83, 052007 (2011)

MiniBooNE was using NUANCE Monte Carlo generator.



MiniBooNE CC π^+ production measurement

A. A. Aguilar-Arevalo et al [MiniBooNE] PRD 83, 052007 (2011)



M. Wilkins, PhD Thesis

Cumulative systematic errors are shown as well.



MiniBooNE SPP data and theoretical models

A comprehensive study was done by Phil Rodrigues, presented at NuInt12.

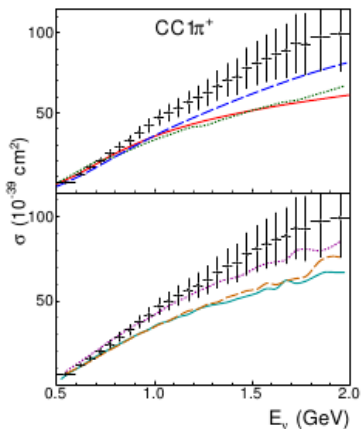
Models

- Hernandez, Nieves, et al
- GiBUU (Mosel et al)
- Athar et al
- Monte Carlo generators: GENIE, NEUT, NuWro.



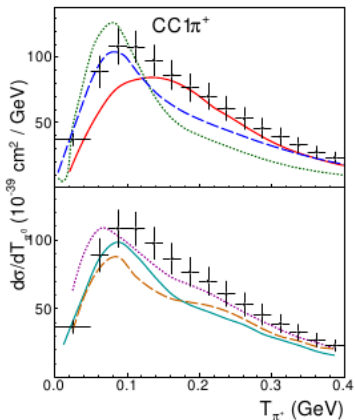
MiniBooNE SPP data and theoretical models

Typically, the measured cross section is underestimated.



— Athar *et al.* Nieves *et al.* - - - GiBUU — NuWro
 GENIE - - - NEUT — MB data

MiniBooNE SPP data and theoretical models (2)

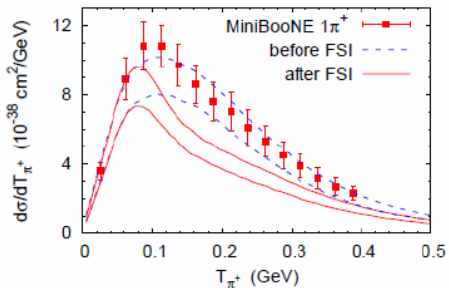


Theoretical models (and MCs) predict a significant hollow at ~ 200 MeV originating from pion absorption.

Remarkably, the measured distribution does not show this feature.

MiniBooNE data and FSI effects

GIBUU results



U. Mosel

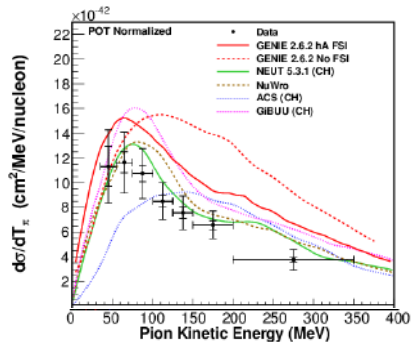
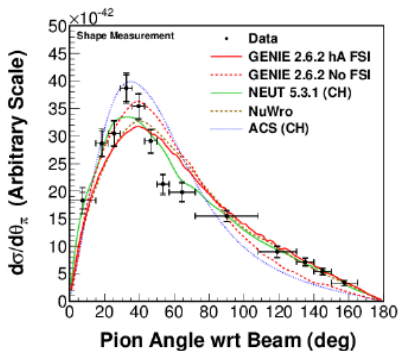
Better agreement with computations without FSI. But we know, FSI must be there.



MINERvA CC π^+ production measurement

- target is CH
- NuMi flux (1.5 – 10) GeV with $\langle E_\nu \rangle \sim 4$ GeV
- a cut $W < 1.4$ GeV
- as a result, the Δ region is investigated, like in the MiniBooNE experiment
- coherent π^+ production is a part of the signal
- signal is defined as $1\pi^+$ and no other π^\pm in the final state
 - contrary to MiniBooNE there can be arbitrary number of π^0 in the final state



MINERvA CC π^+ production measurement

B. Eberly [MINERvA]

B. Eberly [MINERvA]



MinoBooNE and MINERvA

Does it make sense to compare MiniBooNE and MINERvA results?

- very different energy

But...

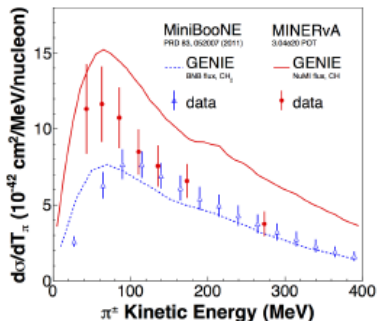
- the same Δ mechanism

The only relevant difference can come from slightly different definitions of the signal, and from relativistic effects.

- at larger energy more momentum is transferred to the hadronic system, and Δ is more relativistic



MiniBooNE and MINERvA



B. Eberly [MINERvA]

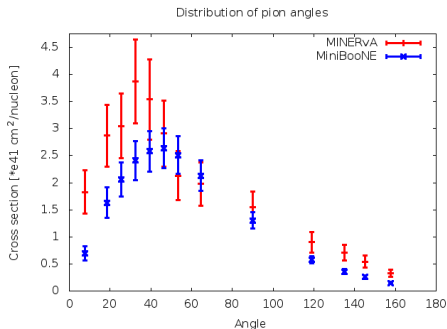
ANL and BNL data suggest that the normalization difference is much larger than 30 – 40%.

Nothing agrees...

- according to GENIE, MINERvA cross section should be \sim twice that large as MiniBooNE, but is not
 - the discrepancy is dramatic for $T_\pi \geq 150$ MeV
- according to GENIE in both cases distributions have peak at ~ 60 MeV, which is the case for MINERvA, but not for MiniBooNE



MiniBooNE and MINERvA



- in M. Wilkins thesis there is distribution in $\cos\theta$
- errors are also taken from M. Wilkins thesis

A general conclusion:

- the shapes are different, mostly at low angles.

Shown for the first time!



MiniBooNE and MINERvA

A possible source of shape difference:

- at larger ν energies Δ moves faster
- the same distribution of π 3-momenta in the Δ rest frame can give different distribution in the LAB frame

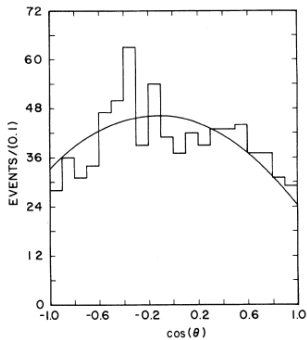
Important to have in MC correct distribution of π^+ angles in the Δ rest frame.



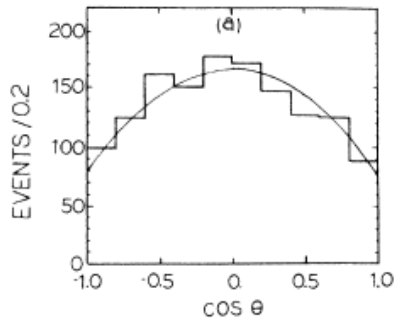
MiniBooNE and MINERvA

What do we know about pion angular distribution?

Below, θ as measured wrt direction of momentum transfer.



ANL



BNL



Conclusions:

- puzzle 1: ANL and BNL normalization
- puzzle 2: neutron versus proton π^+ production
- puzzle 3: MiniBooNE π^+ production data
- puzzle 4: MiniBooNE versus MINERvA π^+ production data

Interesting topic for a discussion



Thank you!

Back-up slides:



Watson theorem

UNITARITY

Writing the S matrix as

$$S = I - iT$$

the unitarity condition $S^\dagger S = I$ that guarantees the conservation of probability implies

$$i(T - T^\dagger) = T^\dagger T$$

For a given transition between asymptotic states $|I\rangle$, $|F\rangle$ one has

$$i\left(\langle F|T|I\rangle - \langle F|T^\dagger|I\rangle\right) = \langle F|T^\dagger T|I\rangle = \sum_N \langle F|T^\dagger|N\rangle \langle N|T|I\rangle = \sum_N \langle N|T|F\rangle^* \langle N|T|I\rangle$$

For the case of $|I\rangle = |F\rangle$ one has

$$\text{Im}\langle I|T|I\rangle = -\frac{1}{2} \sum_N |\langle N|T|I\rangle|^2$$

which constitutes the optical theorem



Watson theorem

Time reversal invariance

Time reversal invariance states that (Time reversal operator \mathcal{T} is antilinear)

$$\langle F|S|I\rangle = \langle I_{\mathcal{T}}|S|F_{\mathcal{T}}\rangle = \langle F_{\mathcal{T}}|S^{\dagger}|I_{\mathcal{T}}\rangle^* = \langle F|\mathcal{T}^{\dagger}S^{\dagger}\mathcal{T}|I\rangle$$

from where

$$\mathcal{T}^{\dagger}S^{\dagger}\mathcal{T} = S \implies \mathcal{T}^{\dagger}\mathcal{T}^{\dagger}\mathcal{T} = T$$

and then

$$\begin{aligned} \sum_N \langle N|T|F\rangle^* \langle N|T|I\rangle &= i\left(\langle F|T|I\rangle - \langle F|T^{\dagger}|I\rangle\right) = i\left(\langle F|T|I\rangle - \langle I|T|F\rangle^*\right) \\ &= i\left(\langle F|T|I\rangle - \langle I|\mathcal{T}^{\dagger}\mathcal{T}^{\dagger}\mathcal{T}|F\rangle^*\right) = i\left(\langle F|T|I\rangle - \langle I_{\mathcal{T}}|T^{\dagger}|F_{\mathcal{T}}\rangle^*\right) \\ &= i\left(\langle F|T|I\rangle - \langle F_{\mathcal{T}}|T|I_{\mathcal{T}}\rangle^*\right) \end{aligned}$$

For the case in which $\langle F|T|I\rangle = \langle F_{\mathcal{T}}|T|I_{\mathcal{T}}\rangle$ and there is only one intermediate state $|N\rangle = |F\rangle$ contributing to the sum one arrives at

$$\langle N|T|N\rangle^* \langle N|T|I\rangle = -2\text{Im}\langle F|T|I\rangle \in \mathbb{R}$$

so that the phases of $\langle N|T|I\rangle$ and $\langle N|T|N\rangle$ coincide. This result constitutes Watson's theorem.

E. Hernandez, CETUP*2014

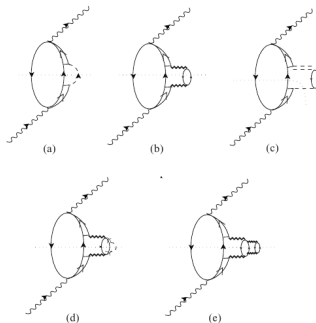
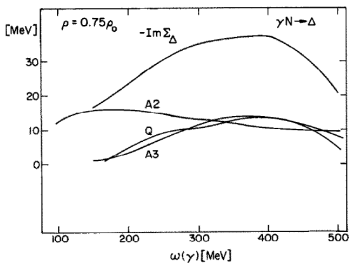


Nuclear target SPP

On theoretical side

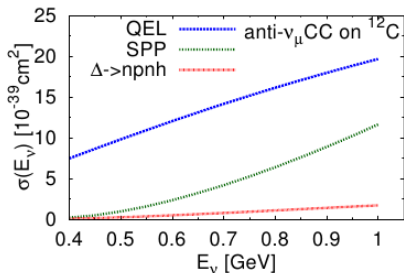
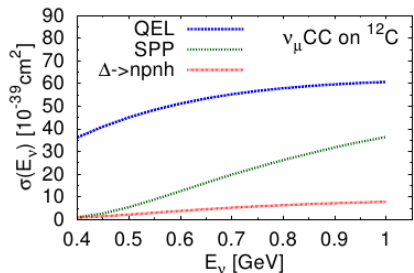
- Δ in-medium self energy; a possibility of $\Delta N \rightarrow NN$ and $\Delta NN \rightarrow NNN$ processes

$$-\text{Im}\Sigma_{\Delta}[\rho(\vec{r})] = C_Q \left(\frac{\rho}{\rho_0}\right)^{\alpha} + C_{A_2} \left(\frac{\rho}{\rho_0}\right)^{\beta} + C_{A_3} \left(\frac{\rho}{\rho_0}\right)^{\gamma}$$



from Oset, Salcedo



Δ in-medium self-energy

from JTS, J. Źmuda

Overall QE, SPP and pionless Δ decay cross sections.

Significant pionless Δ decay contribution and reduction of SPP cross section.

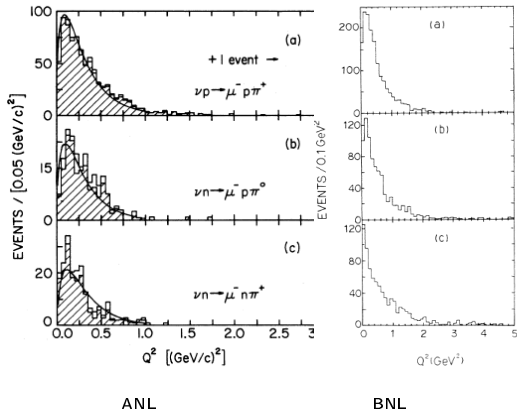
Relativistic evaluation of Δ self-energy was done, but only in infinite nuclear matter.

Virtual Δ and relativity

- assumptions:
target nucleon at rest, at Δ peak
- relativistic factor γ for Δ is:

$$\gamma = \frac{M_{nuc}^2 + M_{\Delta}^2 + Q^2}{2 M_{nuc} M_{\Delta}}$$

- for larger ν energy, larger Q^2 region contributes more, see ANL and BNL example



At MiniBooNE and MINERvA energies the effect is larger.

